Simple emitter patterning of silicon heterojunction interdigitated back-contact solar cells using damage-free laser ablation

Menglei Xu[1,2,*], Twan Bearda[2], Miha Filipič[2], Hariharsudan Sivaramakrishnan Radhakrishnan[2], Ivan Gordon[2], Jozef Szlufcik[2], Jef Poortmans[1,2,3]

[1] *KU Leuven, Kasteelpark Arenberg, 10 B-3001 Heverlee, Belgium*

[2] *Imec, Kapeldreef 75, 3001 Heverlee, Belgium*

[3] *Hasselt University, Hasselt 3500, Belgium*

Abstract:
In early 2017, the world record efficiency for single-junction crystalline silicon (c-Si) solar cells was achieved by merging amorphous silicon (a-Si:H)/c-Si heterojunction technology and back-contact architecture. However, to fabricate such silicon heterojunction interdigitated back-contact (SHJ-IBC) solar cells, complex a-Si:H patterning steps are required to form the interdigitated a-Si:H strips at the back side of the devices. This fabrication complexity raises concerns about the commercial potential of such devices. In this work, a novel process scheme for a-Si:H patterning using damage-free laser ablation is presented, leading to a fast, simple and photolithography-free emitter patterning approach for SHJ-IBC solar cells. To prevent laser-induced damage to the a-Si:H/c-Si heterocontact, an a-Si:H laser-absorbing layer and a dielectric mask are deposited on top of the a-Si:H/c-Si. Laser ablation only removes the top a-Si:H layer, reducing laser damage to the bottom a-Si:H/c-Si heterocontact under the dielectric mask. This dielectric mask is a distributed Bragg reflector (DBR), resulting in a high reflectance of 80% at the laser wavelength and thus providing additional protection to the a-Si:H/c-Si heterocontact. Using such simple a-Si:H patterning method, a proof-of concept 4-cm^2 SHJ-IBC solar cell with an efficiency of up to 22.5 % is achieved.

Keywords: silicon heterojunction, amorphous silicon, solar cells, interdigitated back-contact, laser ablation, patterning

Introduction:

Crystalline silicon (c-Si) PV dominates the current solar-cell market with a market share of more than 90% of the approximately 100 GW_{peak} of PV modules installed in 2017 [1]. To further increase the installation capacity and contribution to global electricity production, the economic competitiveness of commercial c-Si PV with respect to traditional energy sources should be improved. One of the routes is to further raise the energy conversion efficiency of c-Si solar cells, while maintaining a low fabrication cost.

During the past few years c-Si solar cell efficiencies exceeding 25% have been reported by different companies and research institutes (25.1%, Kaneka [2]; 25.2%, Sunpower [3]; 25.6%, Panasonic [4]; 25.7%, Fraunhofer ISE [5]; 26.1%, Fraunhofer ISFH [6]). Notably, all these impressive cell results have been achieved by using passivated contacts, which are either silicon oxide based [6] or low-temperature hydrogenated amorphous silicon (a-Si:H) based, so-called silicon heterojunction (SHJ) technology [7-9]. The excellent a-Si:H/c-Si passivation quality can significantly minimize the minority charge carrier recombination losses at c-Si surface and thus a high open-circuit voltage (V_{oc}) of 750 mV has been achieved [10]. Moreover, interdigitated back-contact (IBC) technology has been widely utilized to maximize short-circuit current density (J_{sc}) [11]. The IBC technology features both electron and hole collection contacts at the rear side of the solar cells, eliminating front grid shadowing and minimizing optical reflection and parasitic absorption losses. This has yielded a high J_{sc} of 42.65 mA/cm^2 [12]. Most recently in early 2017, Kaneka reported the new world record efficiency of 26.7% in a SHJ-IBC solar cell [12].

Although the potential of high efficiency SHJ-IBC solar cells has been demonstrated, commercializing this type of cells still remains challenging. One of the key limitations is that the back-contact scheme requires a sophisticated fabrication process mainly due to the formation of interdigitated p- and n-type a-Si:H strips at the rear side of the device. So far, several a-Si:H patterning approaches have been developed, including photolithography [7, 13-15], screen printing [16], inkjet printing [17], lift-off [14, 18, 19], shadow mask deposition [20-22], and laser ablation [18, 19, 23, 24]. Whereas photolithography is commonly used at laboratory scale, it turns out to be a costly technique and thus not applicable for mass production. Screen printing and inkjet printing are consolidated industrial techniques. However, it still consists of minimum three steps, including an etch resist printing, wet-chemical etching, and resist stripping [16, 17, 20]. In comparison, shadow mask deposition is a simpler method, but it has been reported that special care needs to be taken to reduce several detrimental effects such as a reduction of the a-Si:H deposition rate as well as tapering of the a-Si:H thickness towards the edge of the deposited feature [20, 25, 26]. As an alternative to these patterning methods, laser ablation is a promising industrial-viable approach because of the following three aspects: it is a fast, dry, contactless, maskless, and single side process; it has high process precision; and it permits flexible device design.

In this contribution, we present a photolithography-free process sequence for a-Si:H patterning to form the back-contact architecture by using a damage-free laser ablation and a self-aligned lift-off process. An ultraviolet picosecond laser is utilized to ablate an a-Si:H laser-absorbing layer on top of a stack formed by a dielectric mask/p^+/i a-Si:H/c-Si substrate. The dielectric mask consisting of SiO_x and SiN_x layers forms a distributed Bragg reflector (DBR) to replace the previously reported SiO_x [18, 19], resulting in a high reflectance of 80% at the laser wavelength. This can substantially reduce the laser-induced damage to the underlying a-Si:H/c-Si interface, which is demonstrated by atomic-force microscopy (AFM), photoluminescence (PL) imaging, and Quasi-steady-state photo-conductance (QSSPC) measurements. After laser ablation of the top a-Si:H layer, the dielectric mask and p^+/i a-Si:H stack are patterned by etching. The remaining dielectric mask is used as a sacrificial layer to perform a lift-off process for patterning of the subsequently deposited n^+/i a-Si:H stack. A proof-of concept 4-cm^2 SHJ-IBC solar cell is fabricated using such simple a-Si:H patterning steps, reaching 22.5% efficiency for the best cell.

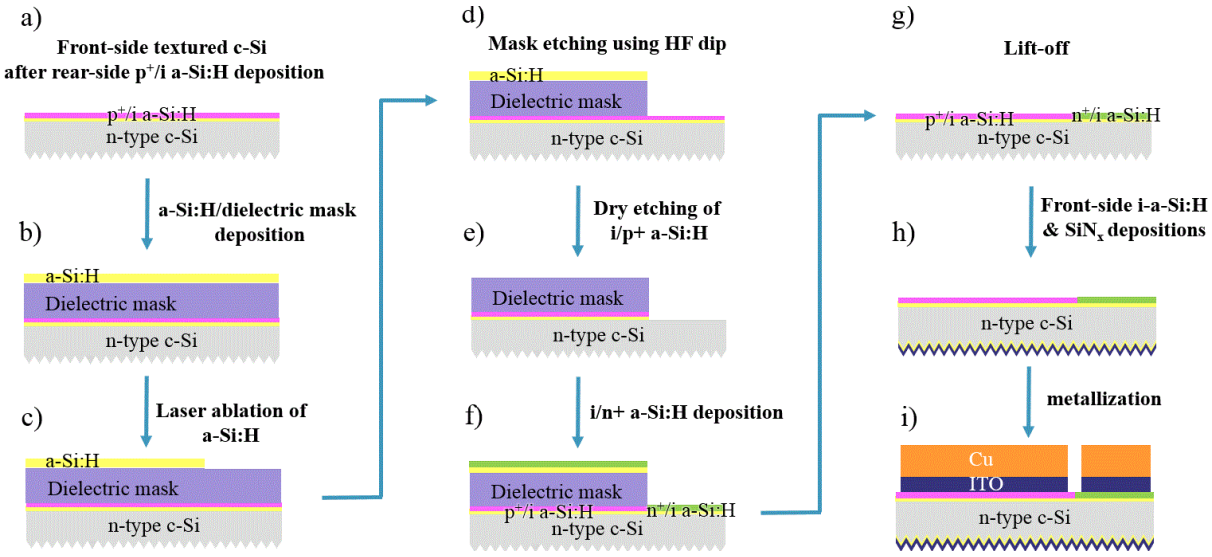

Figure 1 a-i, Cross-sections showing the fabrication process sequence of a SHJ-IBC solar cell using a simple a-Si:H patterning approach based on laser ablation and lift-off. a) Front-side wet-chemical texturing of n-type c-Si and rear-side p^+/i a-Si:H emitter stack deposition. b) dielectric mask and a-Si:H laser-absorbing layer deposition.

c) laser-ablation to remove top a-Si:H absorbing layer according to the predesigned pattern. d) a short wet-chemical etching of the dielectric mask using the laser-patterned a-Si:H as an etch mask. e) NF_3/Ar plasma etching of p^+/i a-Si:H emitter stack using the patterned dielectric layers as an etch mask. The predesigned device pattern is thus transferred to the p^+/i a-Si:H emitter stack. Notably, the non-laser-ablated a-Si:H layer on top of the dielectric mask is etched simultaneously. f) n^+/i a-Si:H BSF stack deposition to re-passivate the etched area. g) a self-aligned lift-off process for n^+/i a-Si:H BSF stack patterning using the patterned dielectric mask as sacrificial layer. h) front-side i-a-Si:H passivating layer deposition and SiN_x deposition as ARC. i) a stack of ITO and Cu deposition, patterned by photolithography.

Process flow of SHJ-IBC solar cell

The 200-μm thick n-type float zone (FZ) monocrystalline silicon wafers (150 mm diameter, <100>, 3 Ω cm) are cleaned and then used for solar cell fabrication. The front side of the wafers is textured in a tetramethyl ammonium hydroxide based solution. The detailed descriptions of wafer cleaning and texturing have been provided elsewhere [14]. According to our device design, approximate 80% of the rear-side device area is covered by the p^+/i a-Si:H emitter stack. We pattern the p^+/i a-Si:H first and thus only 20% of the device area needs to be removed during patterning steps. The fabrication process sequence of a SHJ-IBC solar cell is shown in Figure 1. An p^+/i a-Si:H emitter stack is deposited at the rear side of the wafer using plasma enhanced chemical vapor deposition (PECVD), followed by depositions of the dielectric mask and an a-Si:H laser-absorbing layer of 40 nm. Laser ablation is performed to remove only the top a-Si:H laser-absorbing layer according to the predesigned pattern. An ultrashort-pulsed laser (12 ps, 355 nm, repetition rate of 200 kHz, spot area of 8.33×10^{-7} cm^2, Gaussian distribution profile) with a threshold laser energy fluence of 0.2 J/cm^2 is used in this work. Then the dielectric mask is patterned by a short wet-chemical etching in HF:HCl:H_2O (1:1:20) for 1 min using the laser-patterned absorbing layer as an etch mask. Next, the bottom p^+/i a-Si:H emitter stack is patterned by NF_3/Ar plasma etching using the patterned dielectric layers as an etch mask [27]. The laser pattern is thereby transferred to the p^+/i a-Si:H emitter stack. A blanket n^+/i a-Si:H stack is then deposited by PECVD, and patterned by a lift-off process in HF:HCl:H_2O (2:1:20) for approximately 20 min using the dielectric mask as sacrificial stack, thus eliminating an alignment step [14]. Hence, the interdigitated p^+/i a-Si:H emitter and n^+/i a-Si:H back surface field (BSF) areas are formed using this simple process. Notably, a-Si:H removal in this work is realized by single-side processing, which is either laser ablation or NF_3/Ar plasma etching. Therefore, damage to the front-side pyramids during rear-side a-Si:H patterning steps can be avoided with respect to the methods reported in [18, 19].

At the textured front side, a thin intrinsic a-Si:H passivating layer is deposited and then covered by a silicon nitride (SiN_x) antireflection coating (ARC), yielding good light in-coupling and excellent c-Si surface passivation. In our case, such optimized i-a-Si:H and SiN_x stack results in a front surface recombination velocity *S* as low as 2.6 cm/s at one sun illumination, which are among the best reported *S* values of SHJ solar cells [10, 22]. Such low *S* values are very important to efficiently collect minority charge carriers in IBC solar cells [28, 29].

To finish the device, a stack of indium-doped tin-oxide (ITO) and Cu is deposited at the rear side of the solar cell, and patterned by photolithography and wet chemical etching to form the metal contacts. In this study, the laser line width and line pitch are chosen to match the existing photolithography mask. Nevertheless, the metallization steps can be made upscaled by using either screen printing or inkjet printing to replace photolithography [16, 17, 20, 22]. Thermal annealing at temperatures below 200 °C is applied to the finished cells in order to improve contact behavior.

a-Si:H patterning using damage-free laser ablation

Key to this approach is that laser-induced damage to the p^+/i a-Si:H/c-Si substrate

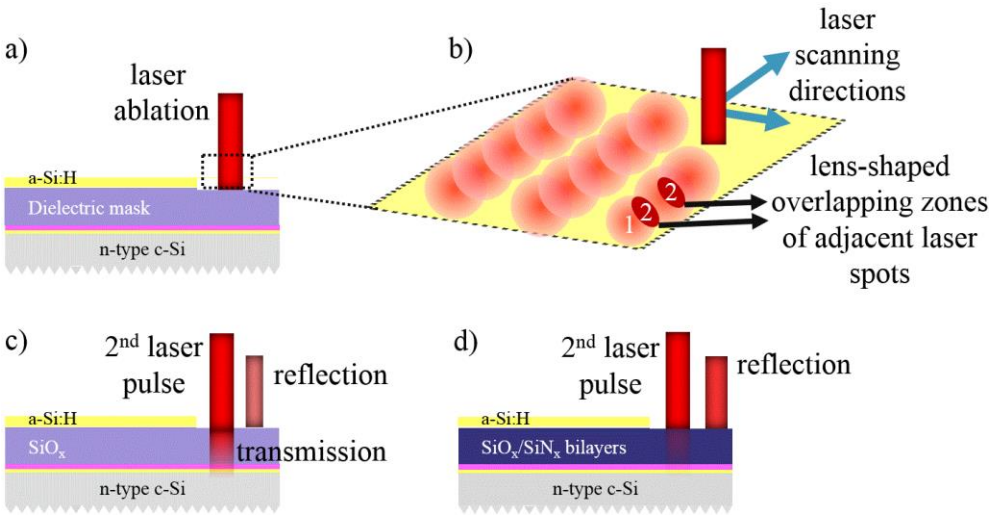

Figure 2 a) cross-sectional view and b) top view of a device wafer after laser ablation. Only the top a-Si:H laser-absorbing layer is removed. Areas 1 and 2 in b) indicate the regions processed by a single laser pulse and two adjacent laser pulses, respectively. The laser light transmissions and reflections in overlapping zones (OZs) on c) SiO_x and d) DBR device wafers during the 2nd laser pulse irradiation. A decreased light transmission through the dielectric mask layers and an increased light reflection are expected on the DBR wafers.

should be substantially reduced or preferably avoided. Several methods have been developed by either optimizing the absorption coefficient of an SiN_x dielectric mask at the laser wavelength, or by using an additional a-Si:H laser-absorbing layer on top of a SiO_x mask [18, 19, 24]. For the latter method, only the top a-Si:H absorbing layer is ablated, shifting part of the laser damage from the bottom p^+/i a-Si:H/c-Si heterocontact to the SiO_x surface. Nevertheless, when scribing line-shaped openings, overlapping zones (OZs), which are irradiated by two adjacent laser pulses, must be considered [18]. As shown in Figure 2 a) – c), after ablation of the a-Si:H absorbing layer by the first laser pulse, the subsequent laser pulse in OZs will transmit through the SiO_x and finally be absorbed by the bottom p^+/i a-Si:H/c-Si. This can result in severe laser damage and thus significant degradation of c-Si surface as well as issues with re-passivation quality [18].

To solve the problem, we propose a novel method of using a more reflective dielectric mask layer to replace the SiO_x layer. In that way, the laser light transmission through the mask and the resulting laser energy absorption in the bottom p^+/i a-Si:H/c-Si can be reduced (see Figure 2 d)). In this work, a stack of alternating SiO_x and SiN_x layers is deposited on p^+/i a-Si:H/c-Si. To form a DBR structure, the required thicknesses of SiO_x and SiN_x layers are determined to be 60 nm and 48 nm, respectively, using optical refractive indices ($n_{SiOx} \approx 1.5$, $n_{SiNx} \approx 1.9$ @ 355 nm) measured by spectroscopic ellipsometry [30, 31]. The SiO_x samples are included as references. As shown in Figure 3, the measured reflectance of SiO_x/p^+/i a-Si:H/c-Si at the laser wavelength of 355 nm is 52%. So approximately half of the laser light that reaches the SiO_x is eventually absorbed by the underlying p^+/i a-Si:H/c-Si due to the transparency of SiO_x at 355 nm. However, the reflectance can be increased to 64% by using one bilayer of SiO_x/SiN_x and further increased up to 80% using five bilayers of SiO_x/SiN_x. Note that the mask in our method is not limited to PECVD SiO_x/SiN_x layers, but can also consist of other layers deposited using other low-cost methods as long as such layers can be easily etched and have the high refractive index difference that is needed to form a DBR [32-37]. Additionally, our approach is also applicable to other laser wavelengths. For instance, the process window with high reflectance can be shifted to other laser wavelengths by simply modifying the thicknesses of the sub-layers in the DBR structure.

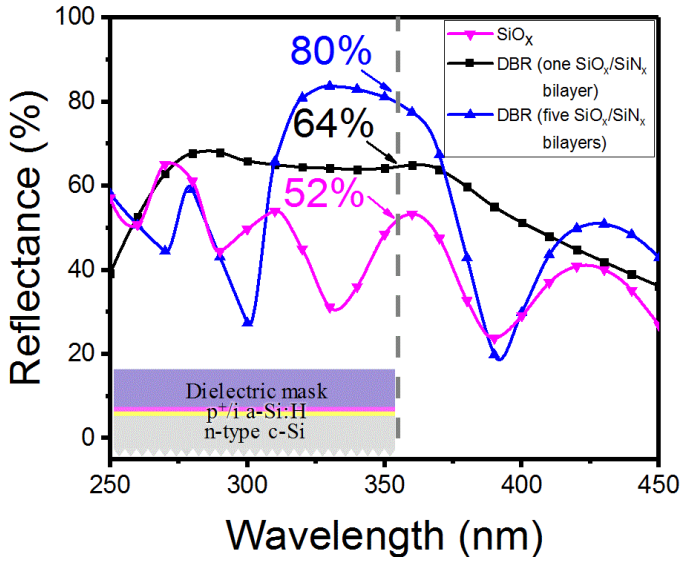

Figure 3 Comparison of the measured reflectance of SiO_x/p^+/i a-Si:H/c-Si and DBR/p^+/i a-Si:H/c-Si. 52% corresponds to the reflectance of the SiO_x sample at the laser wavelength of 355 nm [24]. For DBR samples, the reflectance at 355 nm can be increased to 64% by using one bilayer of SiO_x/SiN_x and further increased up to 80% using five bilayers of SiO_x/SiN_x.

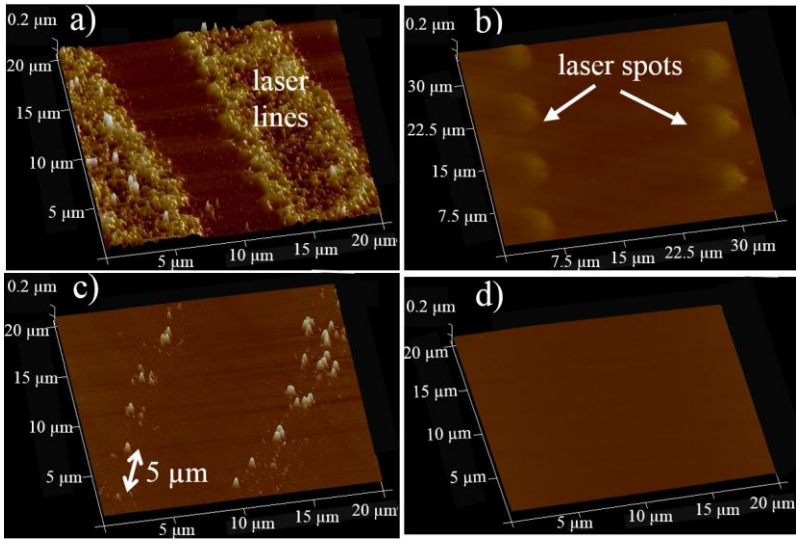

Figure 4 The three-dimensional (3D) AFM images of a-Si:H/SiO_x/p^+/i a-Si:H/c-Si samples after laser ablation at a) 0.7 m/s and b) 2 m/s and subsequent SiO_x mask etching. The 3D AFM images of a-Si:H/DBR/p^+/i a-Si:H/c-Si samples (5 bilayers of SiO_x/SiN_x) after laser ablation at c) 0.7 m/s and d) 2 m/s and subsequent DBR mask etching.

The AFM images of laser-ablated samples after dielectric mask etching are illustrated in Figure 4. For the a-Si:H/SiO_x sample processed by a laser speed of 0.7 m/s, traces of laser-scribed lines are clearly observed in the form of roughness on the p^+/i a-Si:H/c-Si stack as shown in Figure 4 a). This suggests that the laser-induced damage (e.g. roughness, thermal damage) is present not only in OZs but also in the regions irradiated by one laser pulse. Detailed investigation using transmission electron microscopy has been reported by us elsewhere [38]. In short, more severe laser damage is observed in OZs with respect to the regions irradiated by only one laser pulse. When increasing the laser speed to 2 m/s to reduce OZs, separate laser spots are still observed for the a-Si:H/SiO_x sample on the p^+/i a-Si:H/c-Si stack as depicted in Figure 4 b). However, for the a-Si:H/DBR sample consisting of 5 pairs of SiO_x/SiN_x processed at a laser speed of 0.7 m/s, Figure 4 c) shows very limited traces of separate laser spots owing

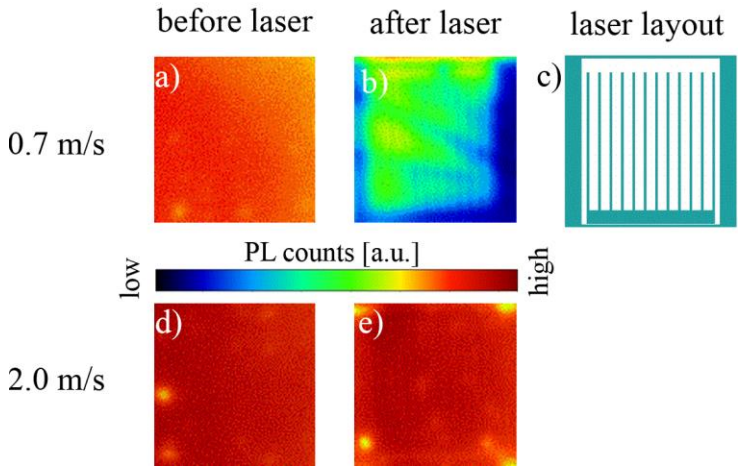

Figure 5 The uncalibrated PL images of DBR device samples (5 bilayers of SiO_x/SiN_x) before and after laser ablation with process speeds of 0.7 m/s and 2.0 m/s, respectively. The green regions in c) indicate the laser-ablated areas. Note the laser layout pattern in c) is visible in the PL image b), corresponding to that of the DBR sample processed by a laser speed of 0.7 m/s.

to the high reflectance of the DBR at 355 nm, which is significantly improved with respect to Figure 4 a). The distance between rough areas is approximately 5 µm, which corresponds to the distance between the OZs. It indicates that laser damage in the regions irradiated by one laser pulse is prevented. The laser damage in OZs can be further reduced by increasing the laser speed to 2 m/s, as shown in Figure 4 d). A smooth surface is achieved, which is improved compared to Figure 4 b) and comparable to the reference c-Si sample without laser ablation process. This means that laser induced roughness might be prevented using the DBR structure and a proper laser speed to reduce OZs, indicating a possible damage-free laser ablation process.

To quantify the impact of laser damage on p^+/i a-Si:H/c-Si passivation quality, uncalibrated PL images are taken and the minority carrier lifetimes (τ) are recorded using QSSPC after p^+/i a-Si:H passivation and after laser ablation, respectively. Results of a-Si:H/SiO_x samples have been discussed in detail by us previously [38]. Comparing Figure 5 a) and 5 b), an p^+/i a-Si:H/c-Si passivation degradation is observed for the DBR device sample processed at a laser speed of 0.7 m/s due to laser damage in OZs. The laser scribed areas with low passivation quality show a pattern, corresponding to the pattern of used laser layout (see figure 5 c). However, when increasing laser speed to 2 m/s, the passivation degradation is diminished as shown in Figures 5 d) and 5 e). To confirm that the passivation is maintained after laser ablation, a square-shaped area (5×5 cm^2) is fully ablated on an a-Si:H/DBR sample utilizing the identical laser condition of 2 m/s. The minority carrier lifetimes τ of the ablated area are measured by aligning QSSPC measurement area and the laser-ablated square. As shown in Figure 6, the lifetimes τ after laser ablation are comparable to the initial τ before laser ablation. This suggests that laser damage introduced to the p^+/i a-Si:H/c-Si heterocontact is prevented, agreeing well with the AFM observations and PL measurements. Several methods capable of reducing laser damage during a-Si:H patterning steps have been reported [18, 19]. Nevertheless, in these methods multiple wet-chemical etching steps of an additional a-Si:H laser-absorbing layer and/or two SiO_2 sacrificial mask layers after laser ablation are always required. In contrast, our approach is simpler because only the DBR sacrificial layers need to be removed by one short HF etching step [39]. It is also worthy to note that although the p^+/i a-Si:H stack in laser processed region is always etched for SHJ-IBC cells fabrication we believe a damage-free laser ablation is still advantageous due to the following two aspects: 1) it allows for wafer screening immediately following laser ablation using PL imaging measurements,

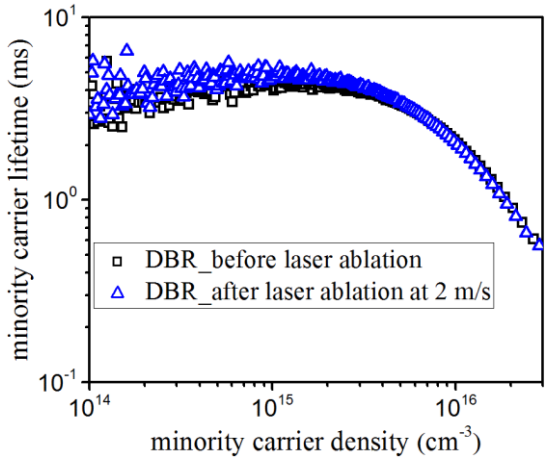

Figure 6 Minority carrier lifetimes τ of the DBR samples (5 bilayers of SiO_x/SiN_x) before laser ablation and after laser ablation at 2 m/s. The lifetimes τ of the ablated area are measured by aligning QSSPC measurement area and laser-ablated square.

Table 1 Summary of the laser-patterned SHJ-IBC cell results

Cells	J_{sc} (mA/cm^2)	V_{oc} (mV)	FF (%)	η (%)
Average of 5	41.5	727	73.6	22.2
Best	41.6	730	74.3	22.5

whereas sacrificial mask etching and re-passivation are needed when the p^+/i a-Si:H passivation stack is damaged by laser ablation (e.g. on SiO_x samples) [38]; 2) it is compatible with another novel a-Si:H patterning method developed by us, where only the doped a-Si:H layer in the a-Si:H passivation stack is etched using NF_3/Ar plasma followed by re-deposition of an a-Si:H layer of an opposite doping type [40]. In this case, we need to ensure that the intrinsic a-Si:H layer on c-Si is not affected by laser damage.

The optimized laser ablation process was then integrated into a process flow (see Figure 1) to fabricate SHJ-IBC solar cells. The cell results are summarized in Table 1. No big difference is observed between the average cell results and the best cell results, indicating a good uniformity of our laser ablation process. A best efficiency of 22.5% with V_{oc} of 730 mV is achieved, which is similar to our best cell fabricated using our photolithography-based baseline process [27]. As far as we know, this is the highest reported efficiency of a SHJ-IBC cell using laser ablation for a-Si:H patterning. In our case, both the photolithography-patterned and the laser-patterned cells efficiencies are mainly limited by low fill factor (FF) values. A breakdown analysis of our photolithography-patterned cells was reported by us previously [14], indicating series resistance R_s as the major loss mechanism. R_s of the laser-patterned cell is estimated by using the parameters from the Suns-V_{oc} pseudo I-V curve (R_s free) and the real light I-V curve (R_s affected) according to [41], as shown in Figure 7. The high R_s value of 1.3 Ω cm^2 is achieved from the laser-patterned cell, comparable to the R_s of 1.6 Ω cm^2 we obtained previously from the photolithography-patterned cell [14]. Notably, all these R_s values are still much higher with respect to the R_s of 0.2 Ω cm^2 calculated from the record SHJ-IBC cell [42]. We are currently optimizing the a-Si:H/ITO heterocontact to improve the contact behavior and thus reduce R_s. Suns-V_{oc} measurements predict that the efficiency of our laser-patterned SHJ-IBC cell can potentially reach 25% by solving the R_s issue.

Conclusion

In this study, we demonstrated a damage-free laser ablation process to significantly

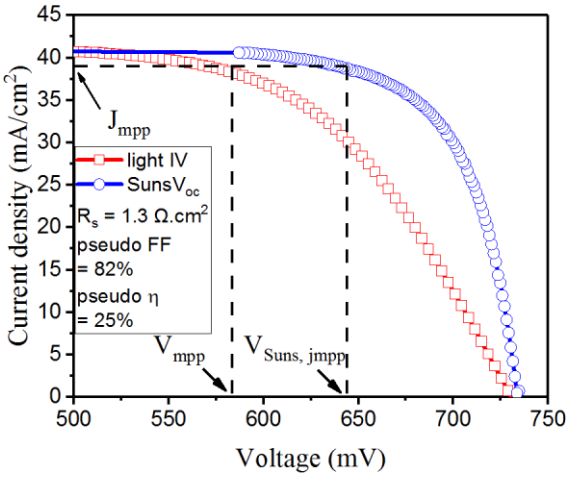

Figure 7 R_s of a laser-patterned SHJ-IBC cell is estimated to be 1.3 Ω cm^2 by using the parameters from the Suns-V_{oc} pseudo *I-V* curve and the real light *I-V* curve. The illumination intensity during Suns-V_{oc} measurement is monitored by a reference cell and the J_{sc} value of Suns-V_{oc} is calibrated using J_{sc} measured from the light *I-V* measurement [43]. The pseudo *FF* (p*FF*) of 82.0% and pseudo efficiency (η) of 25.0% are extracted from the Suns-V_{oc} measurement.

simplify the emitter patterning of SHJ-IBC solar cells. Key to this method is to prevent laser-induced damage to the p$^+$/i a-Si:H passivation layer and c-Si substrate, which is realized using optimized laser conditions and a DBR structure. Therefore, the p$^+$/i a-Si:H/c-Si interface passivation is maintained after laser ablation, as confirmed by PL images and QSSPC measurements. It is worth to note that our approach is also applicable to other laser wavelengths by simply altering the thicknesses of the sub-layers in the DBR structure.

The combination of laser ablation and lift-off results in an alignment-free and photolithography-free a-Si:H patterning process sequence. To demonstrate this developed process, proof-of concept 4-cm^2 SHJ-IBC solar cells have been fabricated on n-type FZ wafers. A best efficiency of 22.5% has been achieved with J_{sc} of 41.6 mA/cm^2 and excellent V_{oc} of 730 mV, similar to that of the best SHJ-IBC cell we obtained previously using the photolithography baseline process for a-Si:H patterning [14, 27]. The current device efficiencies are mainly limited by low *FF* values, which is not related to the developed laser ablation process but due to the high series resistance R_s values. Suns-V_{oc} measurements predict that efficiencies of our SHJ-IBC solar cells using such simple a-Si:H patterning method can potentially reach 25% by solving the R_s issue.

Acknowledgements

The authors gratefully acknowledge the financial support of imec's industrial affiliation program for Si-PV. This project has also received funding from the European Union's Horizon 2020 research and innovation programme under grant agreement no. 727523 (NextBase).

References

[1] Jäger-Waldau, A. *PV Status Report 2017*. *JRC Science for Policy Report* (Publications office of the European Union, 2017).
[2] Adachi, D., Hernández, J. & Yamamoto, K. Impact of carrier recombination on fill factor for large area heterojunction crystalline silicon solar cell with 25.1% efficiency. *Appl. Phys. Lett.* **107**, 233506 (2015).
[3] Green, M. A., Emery, K., Hishikawa, Y.,Warta,W. & Dunlop, E. D. Solar cell efficiency tables (version 47). *Prog. Photovolt. Res. Appl.* **24,** 3–11 (2016).
[4] Masuko, K., Shigematsu, M., Hashiguchi, T., Fujishima, D., Kai, M., Yoshimura, N., Yamaguchi, T., Ichihashi, Y., Mishima, T., Matsubara, N., Yamanishi, T., Takahama, T., Taguchi, M., Maruyama, E. & Okamoto, S. Achievement of more than 25% conversion efficiency with crystalline silicon heterojunction solar cell. *IEEE J. Photovolt.* **4**, 1433-1435 (2014).
[5] Richter, A., Benick, J., Feldmann, F., Fell, A., Hermle, M. & Glunz, S. n-Type Si solar cells with passivating electron contact: Identifying sources for efficiency limitations by wafer thickness and resistivity variation. *Sol. Energy Mater. Sol. Cells* **173**, 96-105 (2017).

[6] Osborne, M. ISFH pushes p-type mono cell to record 26.1% conversion efficiency, PV-Tech (7 February 2018); https://www.pv tech.org/news/isfh-pushes-p-type-mono-cell-to-record-26.1-conversion-efficiency
[7] Nakamura, J., Asano, N., Hieda, T., Okamoto, C., Katayama, H. & Nakamura, K. Development of heterojunction back contact Si solar cells. *IEEE J. Photovolt.* **4,** 1491–1495 (2014).
[8] Yoshikawa, K., Kawasaki, H., Yoshida, W., Irie, T., Konishi, K., Nakano, K., Uto, T., Adachi, D., Kanematsu, M., Uzu, H. & Yamamoto, K. Silicon heterojunction solar cell with interdigitated back contacts for a photoconversion efficiency over 26%. *Nat. Energy* **2,** 17032 (2017).
[9] DeWolf, S., Descoeudres, A., Holman, Z. C. & Ballif, C. High-efficiency silicon heterojunction solar cells: a review. *Green* **2,** 7–24 (2012).
[10] Taguchi, M., Yano, A., Tohoda, S., Matsuyama, K., Nakamura, Y., Nishiwaki, T., Fujita, K. & Maruyama, E. 24.7% Record efficiency HIT solar cell on thin silicon wafer. *IEEE J. Photovolt.* **4**, 96–99 (2014).
[11] Cousins P., Smith D, Luan H, Manning J, Dennis T, Waldhauer A, Wilson K, Harley G & Mulligan W. Generation 3: Improved performance at lower cost. In *Proc. 35th IEEE Photovoltaic Specialist Conf. (PVSC)* 275-278 (2010).
[12] Green M. A., Hishikawa Y., Warta W., Dunlop E. D., Levi, D. H., Hohl-Ebinger J. & Ho-Baillie A. W. H. Solar cell efficiency tables (version 50). *Prog. Photovolt. Res. Appl.* **25,** 668–676 (2017).
[13] Haschke, J., Mingirulli, N., Gogolin, R., Ferré, R., Schulze, T., Düsterhöft, J., Harder, N. & Korte, L. Interdigitated back-contacted silicon heterojunction solar cells with improved fill factor and efficiency. *IEEE J. Photovolt.* **1**, 130–134 (2011).
[14] Xu, M., Bearda, T., Sivaramakrishnan Radhakrishnan, H., Kiran Jonnak, S., Hasan, M., Malik, S., Filipič, M., Depauw, V., Van Nieuwenhuysen, K., Abdulraheem, Y., Debucquoy, M., Gordon, I., Szlufcik, J. & Poortmans, J. Silicon heterojunction interdigitated back-contact solar cells bonded to glass with efficiency >21%. *Sol. Energy Mater. Sol. Cells* **165**, 82-87 (2017).
[15] Granata, S., Aleman, M., Bearda, T., Govaerts, J., Brizzi, M., Abdulraheem, Y., Gordon, I., Poortmans, J. & Mertens, R. Heterojunction interdigitated back-contact solar cells fabricated on wafer bonded to glass. *IEEE J. Photovolt.* **4**, 807-813 (2014).
[16] Thibaut, D., Sylvain, D., Florent, S., Djicknoum, D., Delfina, M., Marie, G., Jean-Paul, K. & Jean, R. Development of interdigitated back contact silicon heterojunction (IBC Si-HJ) solar cells. *Energy Proc.* **8**, 294-300 (2011).
[17] Takagishi, H., Noge, H., Saito, K. & Kondo, M. Fabrication of interdigitated back-contact silicon heterojunction solar cells on a 53-μm-thick crystalline silicon substrate by using the optimized inkjet printing method for etching mask formation. *Jpn. J. Appl. Phys.* **56**, 040308 (2017).
[18] Ring, S., Kirner, S., Schultz, C., Sonntag, P., Stannowski, B., Korte, L. & Schlatmann, R. Emitter patterning for back-contacted Si heterojunction solar cells using laser written mask layers for etching and self-aligned passivation (LEAP). *IEEE J. Photovolt.* **6**, 894-899 (2016).
[19] Harrison, S., Nos, O., D'Alonzo, G., Denis, C., Coll, A. & Munoz, D. Back contact heterojunction solar cells patterned by laser ablation. *Energy Proc.* **92**, 730-737 (2016).
[20] Tomasi, A., Paviet-Salomon, B., Lachenal, D., Martin de Nicolas, S., Descoeudres, A., Geissbuhler, J., De Wolf, S. & Ballif, C. Back-contacted silicon heterojunction solar cells with efficiency >21%. *IEEE J. Photovolt.* **4**, 1046-1054 (2014).
[21] Herasimenka, S. Y., Tracy, C. J., Dauksher, W. J., Honsberg, C. B., & Bowden, S. A simplified process flow for silicon heterojunction interdigitated back contact solar cells: Using shadow masks and tunnel junctions. In *Proc. 40th IEEE Photovoltaic Specialist Conf. (PVSC)* 2486-2490 (2014).
[22] Tomasi, A., Paviet-Salomon, B., Jeangros, Q., Haschke, J., Christmann, G., Barraud, L., Descoeudres, A., Seif, J., Nicolay, S., Despeisse, M., De Wolf, S. & Ballif, C. Simple processing of back-contacted silicon heterojunction solar cells using selective-area crystalline growth. *Nat. Energy* **2**, 17062 (2017).
[23] Xu, M., Bearda, T., Filipic, M., Sivaramakrishnan Radhakrishnan, H., Debucquoy, M., Gordon, I., Szlufcik, J. & Poortmans, J. Damage-free laser ablation for emitter patterning of silicon heterojunction interdigitated back-contact solar cells. In *Proc. 44th IEEE Photovoltaic Specialist Conf. (PVSC)* (2017).
[24] Desrues, T., De Vecchi, S., Souche, F., Munoz, D., & Ribeyron, P. J. SLASH concept: A novel approach for simplified interdigitated back contact solar cells fabrication. In *Proc. 38th IEEE Photovoltaic Specialist Conf. (PVSC)* 1602-1605 (2012).
[25] Ledinský, M., Paviet-Salomon, B., Vetushka, A., Geissbühler, J., Tomasi, A., Despeisse, M., De Wolf, S., Ballif, C. & Fejfar, A. Profilometry of thin films on rough substrates by Raman spectroscopy. *Sci. Rep.* **6**, 37859 (2016).
[26] Paviet-Salomon, B., Tomasi, A., Lachenal, D., Badel, N., Christmann, G., Barraud, L., Descœudres, A., Geissbühler, J., Faes, A., Jeangros, Q. & Seif, J.P. Interdigitated back contact silicon heterojunction solar cells featuring an interband tunnel junction enabling simplified processing. *Sol. Energy* (in press) (2018).
[27] Sivaramakrishnan Radhakrishnan, H., Bearda, T., Xu, M., Jonnak, S. K., Malik, S., Hasan, M., Depauw, V., Filipič, M., Van Nieuwenhuysen, K., Abdulraheem, Y., Debucquoy, M., Gordon, I., Szlufcik, J. & Poortmans, J. Module-level cell processing of silicon heterojunction interdigitated back-contacted (SHJ-IBC) solar cells with efficiencies above 22%: Towards all-dry processing. In *Proc. 43rd IEEE Photovoltaic Specialist Conf. (PVSC)* 1182-1187 (2016).
[28] Lu, M., Bowden, S., Das, U. & Birkmire, R. Interdigitated back contact silicon heterojunction solar cell and the effect of front surface passivation. *Appl. Phys. Lett.* **91**, 063507 (2007).
[29] Hermle, M., Granek, F., Schultz-Wittmann, O. & Glunz, S. W. Shading effects in back-junction back-contacted silicon solar cells. In *Proc. 33rd IEEE Photovoltaic Specialist Conf. (PVSC)* 1–4 (2008).
[30] Palik, E. D. *Handbook of optical constants of solids* (Vol. 3). Academic press. (1998).
[31] Gottschalch, V., Schmidt, R., Rheinländer, B., Pudis, D., Hardt, S., Kvietkova, J., Wagner, G. & Franzheld, R. Plasma-enhanced chemical vapor deposition of SiO_x/SiN_x Bragg reflectors. *Thin Solid Films* **416**, 224-232 (2002).
[32] Someya, T., Tachibana, K., Lee, J., Kamiya, T. & Arakawa, Y. Lasing emission from an $In_{0.1}Ga_{0.9}N$ vertical cavity surface emitting laser. *Jpn. J. Appl. Phys.* **37**, 1424-1426 (1998).
[33] Yokoyama, H., Nishi, K., Anan, T., Yamada, H., Brorson, S. & Ippen, E. Enhanced spontaneous emission from GaAs quantum wells in monolithic microcavities. *Appl. Phys. Lett.* **57**, 2814-2816 (1990).
[34] Anselm, K. A., Nie, H., Lenox, C., Hansing, C., Campbell, J. C., & Streetman, B. G. Resonant-cavity-enhanced avalanche photodiodes grown by molecular beam epitaxy on InP for detection near 1.55 μm. *J. Vac. Sci. Technol. B* **16**, 1426-1429 (1998).
[35] Iga, K. Vertical cavity surface emitting lasers based on InP and related compounds-bottleneck and corkscrew. In *Proc. 8th International Conference on Indium Phosphide and Related Materials (IPRM)* 715-718 (1996).
[36] Wang, Y., Matsuda, O., Serikawa, T., & Murase, K. Raman scattering investigation of the structure of amorphous silicon in a-Si/SiO_2 superlattice films. *J. Phys. IV* **10**, 259-262 (2000).
[37] Heng, C. L., Zhang, B. R., Qiao, Y. P., Ma, Z. C., Zong, W. H., & Qin, G. G. Influences of thicknesses of SiO_2 layers on electroluminescence from amorphous Si/SiO_2 superlattices. *Physica B* ***270***, 104-109 (1999).
[38] Xu, M., Bearda, T., Sivaramakrishnan Radhakrishnan, H., Filipič, M., Gordon, I., Debucquoy, M., Szlufcik, J. & Poortmans, J. Laser assisted patterning of a-Si:H: detailed investigation of laser damage. *Phys. Status Solidi RRL* **11**, 1700125 (2017).

[39] Xu, M., Bearda, T. & Filipič, M. *European patent application No.* 3319132 (2018).
[40] Sivaramakrishnan Radhakrishnan, H., Uddin, MD., Xu, M., Cho, J., Gordon, I., Szlufcik, J. & Poortmans, J. Implementation of a novel silicon heterojunction IBC process flow using partial etching of doped a-Si:H with efficiencies close to 23%. accepted by *35th Eur. Photovoltaic Solar Energy Conf. Exhibit. (EUPVSEC)* (2018).
[41] Wolf, M. & Rauschenbach, H. Series resistance effects on solar cell measurements. *Adv. Energy Convers.* **3**, 455-479 (1963).
[42] Yoshikawa, K., Yoshida, W., Irie, T., Kawasaki, H., Konishi, K., Ishibashi, H., Asatani, T., Adachi, D., Kanematsu, M., Uzu, H. & Yamamoto, K. Exceeding conversion efficiency of 26% by heterojunction interdigitated back contact solar cell with thin film Si technology. *Sol. Energy Mater. Sol. Cells* **173**, 37-42 (2017).
[43] Sinton, R. A. & Cuevas, A. A quasi-steady-state open-circuit voltage method for solar cell characterization. In *Proc. 16th Eur. Photovoltaic Solar Energy Conf. Exhibit. (EUPVSEC)* 1152–1155 (2000).